Modeling of Suspension Flow in Pipes and Rheometers

Nicos S. Martys[1], Chiara F. Ferraris[1], and William L. George[1]

[1]National Institute of Standards and Technology

Abstract Measurement and prediction of the flow of suspensions like fresh concrete represents a significant challenge for both the experimentalist and modeler. In this paper, results of a computational study of suspension flow in a pipe and a rheometer design using a four blade vane as an impellor are given. The computational method is based on the Smooth Particle Hydrodynamics approach. Flow fields and the spatial distribution of solid spherical inclusions for the case of pipe flow will be shown as a function of the matrix fluid properties, (including Newtonian, shear thinning and shear thickening), driving force, and volume fraction of particles. A strong effective slip phenomenon is shown for the case of a suspension with a shear thinning fluid matrix. Results will be compared to experiments. Aspects of shear induced migration in a vane rheometer and its effects on rheological measurements will be briefly discussed.

Keywords: Rheology, Concrete, Non-Newtonian, Smoothed Particle Hydrodynamics

Introduction

The flow of suspensions is of fundamental interest and plays an important role in a wide variety of technical applications including paints, cement based materials, slurries, and drilling fluids [1]. A suspension can be described as a collection of solid inclusions embedded in a fluid matrix. Measuring and predicting the flow of suspensions remains a great scientific challenge. Suspensions can be quite complex as the inclusions may have a wide range of shapes and a broad size distribution. Further complicating matters is that different matrix fluids may have quite disparate flow behaviour. While the simplest type of matrix fluid is Newtonian, where the local stress is proportional to the shear rate, the matrix fluid can exhibit quite complex behaviour including shear thinning (viscosity decreases with shear rate), shear thickening (viscosity increases with shear rate), viscoelastic, or even have a time dependence. In this paper, results will be presented from numerical simulation of the flow of suspensions in a pipe geometry where the matrix fluid is either Newtonian, shear thinning, or shear thickening. Flow fields and the spatial distribution of neutrally buoyant solid spherical inclusions for the case of pipe flow will be shown as a function of the matrix fluid properties. In addition, a brief discussion of suspension flow in a vane rheometer, illustrating shear induced migration will also be given.

Computational Model

The computational approach utilized in this work, for modeling suspension flow, is based on the Smoothed Particle Hydrodynamics (SPH) method [2]. A full description of SPH is beyond the scope of this paper. A detailed description of this model is given in Martys et al. [3]. For this paper let it suffice to say SPH is a Lagrangian formulation of the Cauchy momentum equation that has been adapted to model generalized Newtonian fluids (where the viscosity is shear-rate dependent) and the motion of rigid bodies. In addition, this approach has been extended to include lubrication forces in order to properly model interactions between solid spherical inclusions when they are in very close proximity. The simulation code utilized for this work has been validated for a variety of flow scenarios (Fig.1) where excellent agreement with analytic solutions is found of flow fields for non-Newtonian continuum fluids in channel and tube geometries and flow of suspensions with power law matrix fluids in a Couette geometry [3].

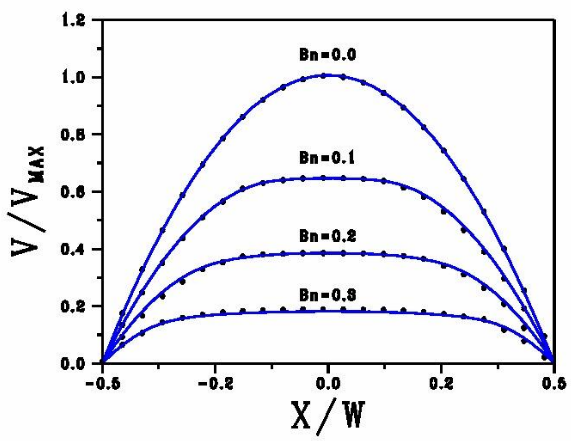

Figure 1. Velocity profiles for flow of non-Newtonian fluid in a 2D channel of width, W, driven by a body force. The fluid properties are based on an approximation of the Bingham model of Papanastasiou [3,4]. For Bingham number Bn =0, the fluid is Newtonian. As Bingham number is increased the fluid more closely approximates a Bingham fluid. The solid lines are from solution of the generalized Navier-Stokes equations using this model and the points are from the simulation.

Pipe Flow: Model

Several assumptions were made to model suspension flow in a pipe. For simplicity, a gravity driven flow is assumed. Periodic boundary conditions at the inlet and outlet are observed (Fig.2). When modelling lubrication forces between a sphere and a pipe wall, the pipe wall is assumed to be a plane locally. As long as the radius of the sphere is much smaller than the pipe radius this approximation should hold. For our simulations, the radius of the sphere is less than a factor 1/32 of the pipe radius. In addition, this relative size is not too far off from what would be associated with a sand particle in a one inch (0.0254 m) pipe which is commonly used for pumping grouts.

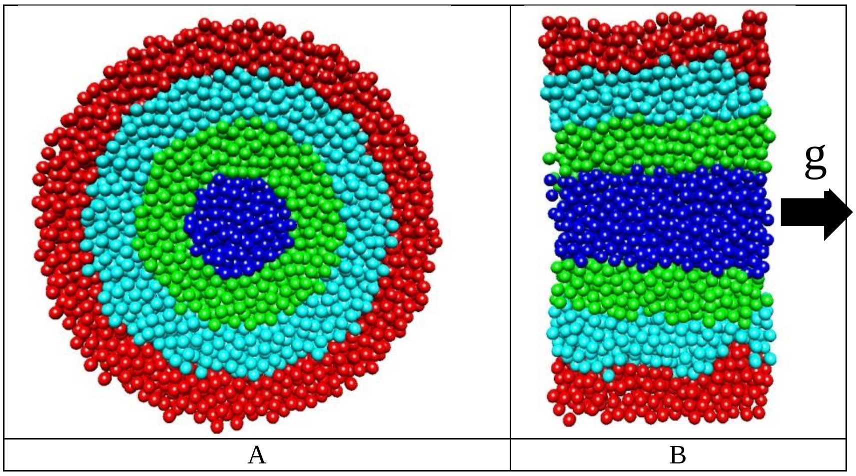

Figure 2. Cross sections of suspension in pipe flow. The solid volume fraction is 40 %. The colors correspond to the initial radial position of the spheres.

In this paper, three types of matrix fluids will be considered: shear thinning, shear thickening and Newtonian (Fig.3). For the model fluids used in this paper, all three behave as a Newtonian fluid in the low shear rate regime. However, at high shear rates the shear thinning and shear thickening fluids behave as power-law fluids with the viscosity scaling as $\dot{\gamma}^{-0.5}$ and $\dot{\gamma}^{0.5}$ respectively, where $\dot{\gamma}$ is the shear rate. A no slip boundary condition is assumed throughout all the simulations (i.e., the fluid velocity is zero at the pipe wall).

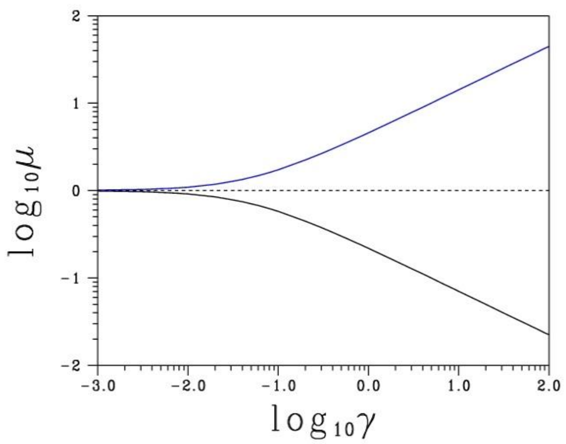

Figure 3. Viscosity vs. shear rate for matrix fluids studied. The Newtonian fluid is the dashed line. The shear thinning ($\mu \sim \dot{\gamma}^{-0.5}$ at high shear-rates) and shear thickening thinning ($\mu \sim \dot{\gamma}^{0.5}$ at high shear-rates) fluids are shown as the solid black and blue lines respectively.

Simulations Results: Pipe Flow

Consider the case of a pipe flow of a suspension in a Newtonian fluid matrix. Fig. 4A shows the velocity profiles for suspensions with volume fraction 20 % and 50 %. Also, for comparison, the flow field for the case of volume fraction 0 % is included. For each volume fraction, the velocity is scaled by the maximum velocity reached in the simulation. It is observed that as volume fraction is increased the velocity profile becomes flatter in the centre of the pipe. This is due to an increase (Fig. 4B) in the density of spheres in the centre of the pipe due to a shear induced migration. Such migration has been observed experimentally [5, 6, 7] and in quasi 2D flow simulations of channel flow using Stokesian Dynamics [8]. Although not clearly seen in the Stokesian dynamics simulations, it was found that, at high volume fractions there is a tendency for structure to develop at fairly large length scales. This is partly due to a local crystallization effect that is known for the case of monosize hard spheres where the volume fraction is approximately 49 % or higher. This phenomenon was observed in experimental data [5] as well.

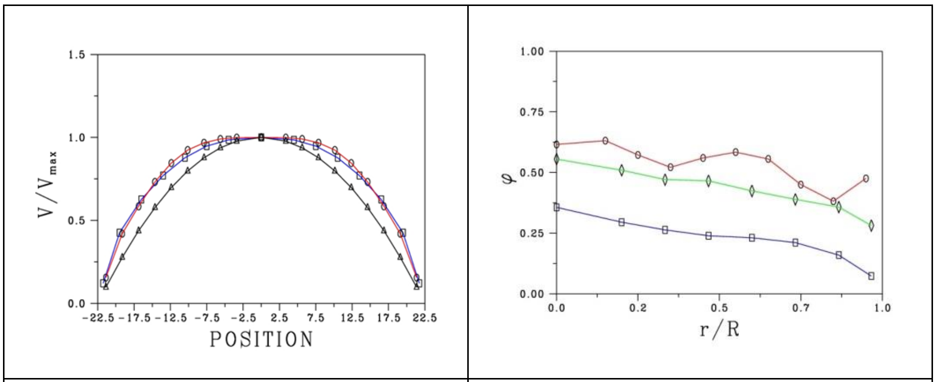

A	B

Figure 4. A) Rescaled velocity profiles for pipe flow of suspension with Newtonian fluid matrix in pipe for particles volume fractions 0 % (triangles), 20 % (squares), and 53 % (circles). As particles volume fraction increases the flow profiles flatten, deviating from parabolic, as found for pipe flow of a Newtonian fluid. B) Radial dependence of the local volume fraction for suspensions with volume fraction 20 % (squares), 40 % (diamonds) and 53 % (circles). At low volume fraction the local volume fraction decreases from the centre of the pipe. At high volume fractions there is still a radially decreasing trend in density, however, there are indications of a long range order in the density profile.

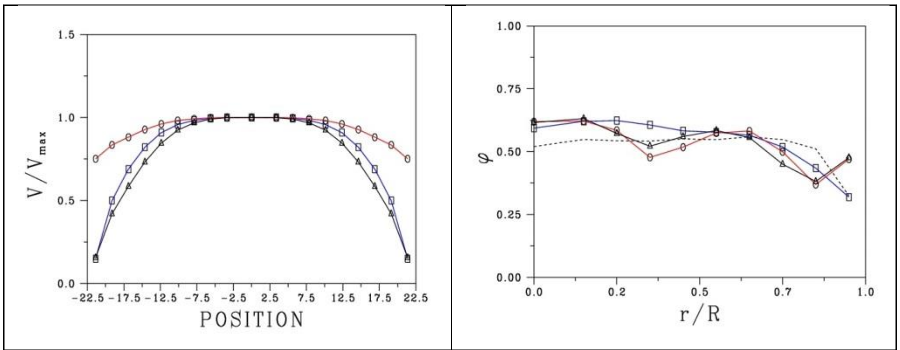

A	**B**

Figure 5. A) Comparison of rescaled velocity profiles for Newtonian (triangles), shear thickening (squares), and shear thinning (circles) fluids. Volume fraction of spherical inclusion is 53 %. A strong effective slip near the pipe surface is observed for the suspension with shear thinning fluid matrix. B) Comparison of the radial dependence of the local volume fraction for suspensions with volume fraction 53 % and different fluid matrices, Newtonian (triangles), shear thickening (squares), and shear thinning (circles). The dashed line indicates the initial radial dependence for all three simulations.

Suspensions flow with a shear thinning, shear thickening, and Newtonian fluid matrices was examined. Figure 5A shows the scaled velocity profile for each type of matrix fluid. Clearly, the velocity profiles are quite different depending on the fluid matrix. Both the shear thinning and shear thickening cases appear to have a more flattened velocity profile than with a Newtonian matrix. Most interesting is the appearance of a strong effective slip for the case of the shear thinning matrix. In the simulation code, there is an enforcement of no slip boundary condition at the pipe wall. However, for spheres near the pipe wall there is a very high shear rate leading to a very low viscosity. Hence, the spheres can move quite easily near the pipe wall giving an appearance of a slip effect. Figure 5B shows the density profile for the three matrix fluids. Both the Newtonian and shear thinning fluids show the development of a long range order as seen in the oscillation of the density. However, the shear thickening fluid did not exhibit this behaviour. This may be a consequence of the system having not evolved for a long enough period of time for this structure to develop. Indeed, any lateral motion for the shear thickening matrix fluid appeared to be significantly suppressed due to the shear thickening behaviour of the matrix fluid.

All simulations in the low Reynolds number (Re) regime exhibited evidence of shear induced migration [9] towards the central axis of the pipe. Such phenomena are described by the suspension balance and related continuum models [8, 9, 10, and 11]. Reasonable estimates of the radial dependence of the density may be obtained for low to moderate volume fractions, although the exact structure observed in experiment and our simulations at high volume fractions would be difficult to recover by these approaches without further modification. For the case of a shear thinning fluid matrix, single phase continuum models may under predict the total mass flow because the effective slip, as seen in Fig. 6, may not be properly accounted for. Also, for the case of shear thickening fluid matrix, a single phase continuum prediction of flow would be higher in comparison to this simulation because any additional increase of local shear rates due to the proximity of spheres at the wall surface make the viscosity higher and hence restrict flow.

Simulations Results: High Reynolds Number Flow

As Re is increased, inertial forces are expected to play a more important role. To illustrate this, consider the case where Re is approximately 3000 for a dilute suspension with volume fraction 5 %. Figure 7A shows a succession of velocity profiles for this system. Note the slight inflection of the velocity profile not far from the pipe wall. This is an artefact of inertial forces playing a role, overcoming the shear induced forces, such that the spheres begin to form a ring near the pipe wall (Figure 7B). Such behavior has been observed in high Re flow in pipe systems [7]. It should be pointed out that the final velocity profile, shown is not an equilibrium profile as this simulation had not progressed long enough to reach that stage. However, it had reached a sufficient state as to illustrate the effect of high Re flow.

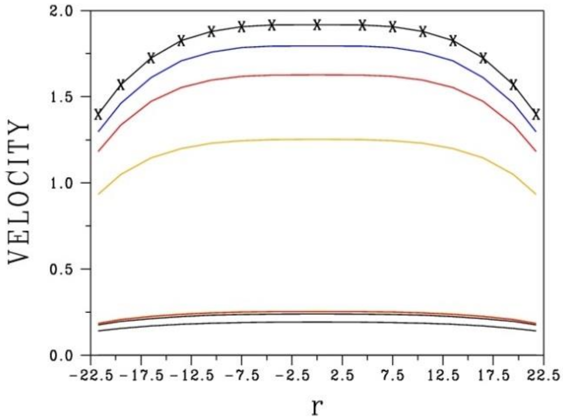

Figure 6. Snap shots of the time evolution of velocity profiles for two body forces g (lower set of curves) and 3g (upper set of curves) for the case of a suspension with volume fraction 53 % and shear thinning matrix. The effective slip is enhanced with increasing body force and roughly scales as g squared for this shear thinning fluid.

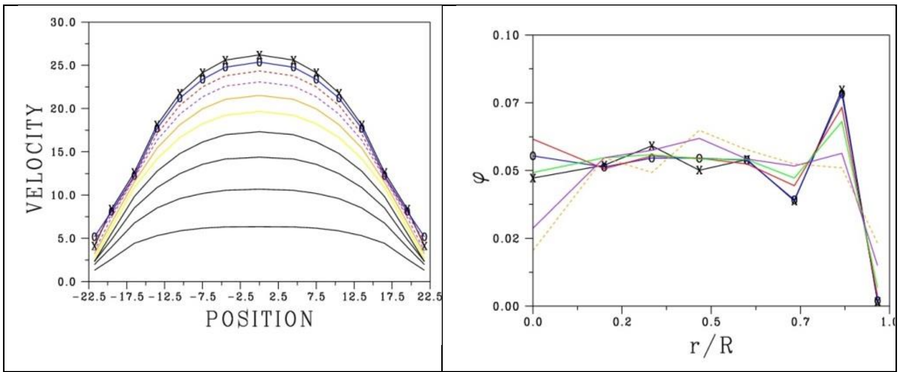

A	B

Figure 7. A) Snapshots of the time evolution of velocity profiles for suspension with volume fraction 5 %, Newtonian fluid matrix and Re increasing to approximately 3000. Note the velocity profiles deviate from parabola as Re increases during the evolution of flow. B) Time evolution of the radial dependence of the local volume fraction for suspensions with volume fraction 5 %, Newtonian fluid matrix. The dashed line indicates the initial local volume fraction. The curves marked with the circle and X correspond to the velocity profiles shown in Fig. 7B. Note the density increase near the pipe wall and a secondary ring of spheres developing near r/R=.3.

Simulations Results: Vane Rheometer

Here, the effect of shear induced migration in a vane rheometer is examined. The vane rheometer is commonly used for determining the viscosity of fluids (Fig.8A) such as concrete. Often one approximates the vane as a cylinder and assumes a coaxial geometry to estimate the viscosity of the fluid. Making this assumption will result in underestimating the value of viscosity, depending on the number of blades in the vane. However, there are analytically determined corrections, based on a continuum fluid approximation (i.e. no solid inclusions) that can help compensate for this assumption. Unfortunately, when the fluid is a suspension, other factors contribute to an even lower viscosity measurement. In our simulations, this behaviour can be attributed to the migration of particles from the blade and towards the wall as shown in Fig. 8C. Such migration outward movement can lead to considerably lower estimates of the of the suspension viscosity due to the decreased coupling of the rotator and the suspension. It was found that estimates of viscosity based on the vane simulations were a factor of two lower than that obtained from simulations using a Couette geometry. It should be pointed out that the migration observed here may be mitigated depending on the nature of the matrix fluid, volume fraction of solids, particle size distribution, vane design and applied torque.

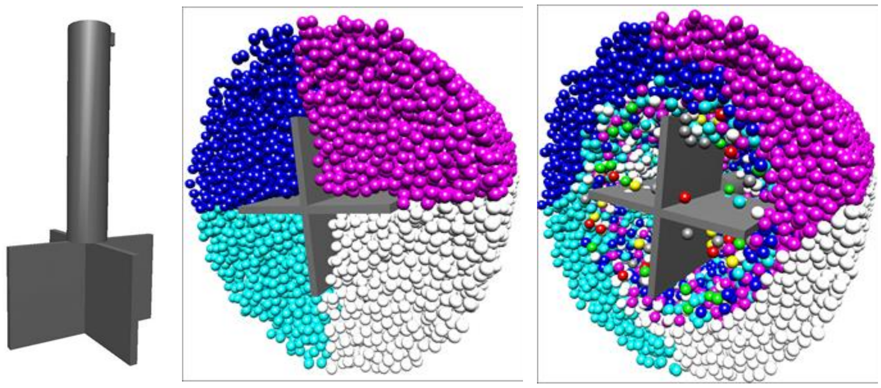

A B C

Figure 8: A) Four blade rheometer vane. B) and C) show the cross section of the vane in a suspension: B) initial (B) and C) late stage (over 20 full rotations of the vane). Note that many of the spheres have been driven outside the inner region of the blade. Sphere volume fraction is 40 %.

Conclusions

In this paper, the utility of modelling suspension flow in a variety of geometries was demonstrated. Specifically, computational modelling can help develop fundamental insights into physical mechanisms, such as the role of shear induced migration and inertial forces that influence flow and effect the interpretations of measurements in these flow geometries. Further, such knowledge can help provide insight about how to tailor mix designs for optimal flow properties in order to reduce cost in placement of concrete and to improve its performance.

Acknowledgements

The authors would like to gratefully acknowledge support from the Sustainable Materials Program at NIST. An award of computer time was provided by the Innovative and Novel Computational Impact on Theory and Experiment (INCITE) program. This research used resources of the Argonne Leadership Computing Facility, which is a DOE Office of Science User Facility supported under Contract DE-AC02-06CH11357.

References

[1] Larson, R.G., *The structure and rheology of complex fluids*, (Oxford University Press, New York, 1999).
[2] Monaghan, J. J., (2005), *Rep. Prog. Phys.*, vol. 68, p. 1703.
[3] Martys, N. S., George, W. L., Chun, B. W., Lootens, D., (2010), *Rheol. Acta*, vol. 49, p. 1059.
[4] Papanastasiou, T.C., (1987*)*, *J. Rheol*., vol. 31, p.385.
[5] Hampron, R. E. and Mammoli, A. A. , (1997), *J. Rheol,* vol. 41, p. 621.
[6] Lyon, M. K.. and Leal L.G., (1998), *J. Fluid Mech.*, vol, 363, p. 25.
[7] Matas, J.P., Morris, J.F., and Guazzelli, *Oil and Gas Science Technology. – Rev. IFP*., (2004), vol 59 No.1. p.59.
[8] Nott, P.R., and Brady, J.F., (1994), *J. Fluid Mech*., vol. 275, p. 157.
[9] Morris, J.F. and Boulay, F., ((1999), *J. Rheol*., vol. 43, p. 1213.
[10] Leighton, D. and Acrivos A., (1987), *J. Fluid Mech.*, vol, 181, p. 415.
[11] Zarraga, I.E., Hill, D.A., and Leighton, D.T. (2000), *J. Rheol*., vol. 44, p.185.